Laboratori Nazionali di Frascati

LNF-68/69

G. Barbiellini, G. Capon, G. DeZorzi and G. P. Murtas : PROTON COMPTON EFFECT BY POLARIZED PHOTONS AT 90° IN THE C. M. SYSTEM IN THE FIRST RESONANCE REGION.

Estratto da : Phys. Rev. 174, 1665 (1968)

Reprinted from THE PHYSICAL REVIEW, Vol. 174, No. 5, 1665–1673, 25 October 1968
Printed in U. S. A.

Proton Compton Effect by Polarized Photons at 90° in the c.m. System in the First Resonance Region

G. BARBIELLINI, G. CAPON, G. DE ZORZI, AND G. P. MURTAS
Laboratori Nazionali di Frascati del CNEN, *Frascati, Rome, Italy*
(Received 24 April 1968)

For the reaction $\gamma+p\rightarrow\gamma'+p'$ (proton Compton effect), we have measured the ratio $d\sigma_{\parallel}/d\sigma_{\perp}$ between the cross sections for linearly polarized photons, using the coherent bremsstrahlung beam of the Frascati electron synchrotron. At 90° in the c.m. system and in the photon energy region $300\leq K\leq 335$ MeV, we find $d\sigma_{\parallel}/d\sigma_{\perp}=2.1_{-0.4}^{+0.5}$. In the absence of theoretical predictions based on the dispersive theory in this energy region, this result is compared with the values obtained using an isobaric model, taking into account various possible intermediate states.

I. INTRODUCTION

POLARIZATION of a γ-ray beam[1] can provide further information on γ-induced reactions. A polarized beam is a facility of the Frascati 1-GeV electron synchrotron and a considerable amount of investigation on the pion photoproduction has already been carried out with it.

Experimental data on pion photoproduction cross sections are now relatively numerous and accurate, and information on production from polarized beams and on the polarization of the recoil nucleon is coming out. Moreover, in these last years agreement between theory and experiment has gradually improved as a result of progress achieved on both sides. Nowadays there are many improvements on the original Chew-Goldberger-Low-Nambu (CGLN) theory of photoproduction which are in satisfactory agreement with the most refined experimental data.

For the Compton effect, the experimental data are less abundant and precise and are restricted to the measurement of the cross sections; no experiments with polarized photons or on the recoil nucleon polarization have been done. The comparison between theory and experiment, which has been mainly made with dispersion-theory techniques and with the isobaric model, is not as satisfactory as in photoproduction.

It is then convenient to increase and improve the experimental data, in order to develop a more stringent comparison between theory and experiment for the Compton effect. This can contribute to a better understanding of electromagnetic interactions of hadrons. We have therefore measured the quantity $R_\sigma=d\sigma_{\parallel}/d\sigma_{\perp}$, where $d\sigma_{\parallel}$ ($d\sigma_{\perp}$) is the cross section for Compton scattering with the incoming photon polarized parallel (normal) to the reaction plane. The experiment is made at 90° in the c.m. system, and the R_σ value is given for the energy interval 300–335 MeV of the primary photon, where the beam polarization attains its maximum.

[1] G. Barbiellini, G. Bologna, G. Diambrini, and G. P. Murtas, Phys. Rev. Letters 8, 112 (1962).

II. BEAM CHARACTERISTICS

The experiment has been performed using a polarized γ-ray beam, which is obtained using a diamond crystal as radiator. The properties of such a beam have been described in Ref. 1. The crystal is oriented in such a way that the electron momentum **p** lies in the plane of the [110], [001] axes, at a small angle with respect to the [110] axis. Then the beam spectrum presents an intensity peak, to which corresponds also the maximum polarization, at a photon energy dependent on the angle θ between **p** and the [110] axis.

The polarization is defined as

$$P(K)=[I_n(K)-I_p(K)]/[I_n(K)+I_p(K)],$$
$$K=\text{photon energy},$$

I_n (I_p) being the intensity of photons with electric vector normal (parallel) to the [110]-[001] plane.

Data are collected using two diamonds: The plane [110]-[001] is vertical for the first one, horizontal for the second one. In the first (second) case we have an excess of photons with polarization vector parallel (normal) to the reaction plane, which is horizontal in our experiment. If $C_{\parallel}$, $C_{\perp}$ are, respectively, the Compton counting rates for the two situations, one obtains the cross-section ratio via the formula

$$\frac{d\sigma_{\parallel}}{d\sigma_{\perp}}=\frac{|P|(R_c+1)+(R_c-1)}{|P|(R_c+1)-(R_c-1)},\quad R_c\equiv\frac{C_{\parallel}}{C_{\perp}}. \qquad (1)$$

During the experiment the beam spectrum has been measured with a pair spectrometer of energy resolution $\Delta K/K=\pm 4\%$. The beam dose is measured with a Wilson quantameter. In Fig. 1 are shown the spectra for the two diamonds as measured with the pair spectrometer. Each one is the weighted mean of various measured spectra; the slight difference between them is due to the impossibility of reproducing exactly every time the position of the crystal. In the following, the counting rates are properly corrected for the small differences in the intensities.

For any orientation of the diamond it is possible to calculate theoretically the beam spectrum and polarization. Figure 2 shows the average experimental spectrum,

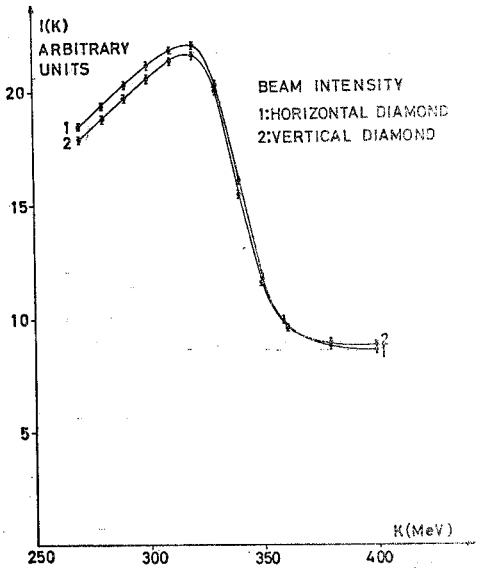

FIG. 1. Behavior of the experimental beam intensity $I(K)$ as a function of the photon energy K for the two diamonds. $I(K)$ is defined as $I(K)=N(K)K$, where $N(K)$ is the number of photons per unit energy interval.

together with the theoretical spectrum which is in agreement with it. The theory takes into account the experimental atomic form factor, Molière multiple scattering in the diamond, electron-beam angular divergence, collimation, and the energy resolution of the pair spectrometer. In addition, the theoretical polarization associated with this theoretical spectrum is shown. This polarization is assumed to be the beam polarization. This general procedure for obtaining a reliable value of the polarization has been devised by Bologna.[2] The error in the polarization may be due as much to the approximations which are present in the calculus, as to statistical uncertainties in fitting the experimental spectrum. As a reasonable estimate we have assumed $\Delta P=0.01$.

Finally, we remark that the K interval where the polarization is high enough to allow a measurement of $d\sigma_{\parallel}/d\sigma_{\perp}$ with reasonable error is relatively small, about 80 MeV. Therefore it is not possible to obtain the energy dependence of $d\sigma_{\parallel}/d\sigma_{\perp}$ without changing the setting of the diamond.

III. EXPERIMENTAL SETUP

The observation of the Compton effect is made difficult by the presence of π^0 photoproduction. We separate Compton and π^0 events, following a method previously used by Stiening *et al.*[3] comparing the measured photon direction with the one expected according to Compton kinematics. In order to accomplish this, our experimental apparatus measures both the direction and the energy of the proton, and the photon direction.

The experimental setup is shown in Fig. 3. The target is a liquid-hydrogen cell of 3×3-cm^2 cross section and 15-cm length. At 44° with respect to the beam direction we have the proton telescope. It consists of two thin-plate spark chambers for direction measurement and of a 20-gap range spark chamber of total thickness $21\times0.5=10.5$ mm of aluminum. Plastic counters S_1, S_2, and S_3 define a stopped proton according to the electronic block diagram of Fig. 4. The S_1

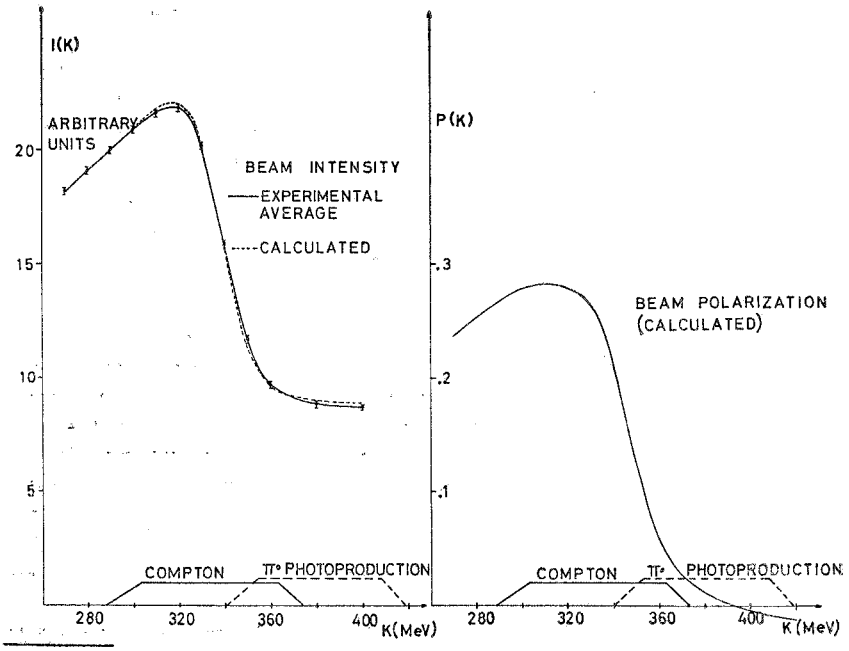

FIG. 2. Behavior of the beam intensity averaged over both diamonds and of the corresponding polarization $P(K)$ as a function of the photon energy K. Along the K axis are shown the intervals which contribute, in our experimental conditions, to the Compton effect and π^0 photoproduction. The trapezoidal shape shows efficiency behavior due to target thickness.

[2] G. Bologna (to be published).
[3] R. F. Stiening, E. Loh, and M. Deutsch, Phys. Rev. Letters 10, 536 (1963).

pulse height is analyzed and the S_1S_2 photomultiplier voltages are adjusted in order to have small pion contamination. Along the proton path we have two helium bags to decrease proton scattering and therefore the error in its direction.

In the photon direction (75° from the beam), we have a veto plastic counter A, a shower spark chamber, and an integral lead glass Čerenkov counter $\check{C}$. The shower spark chamber has two thin Al plates followed by 19 thick plates (each one being a sandwich of 1-mm Al and 0.5-mm Pb), and finally by two additional thin Al plates. With it we determine first the conversion point of the photon and then its direction joining this with the target point obtained extrapolating the proton direction backwards. The conversion efficiency of the shower spark chamber is about 70%. The master pulse which triggers all the spark chambers is given by $T+\check{C}+\bar{A}$ (see the electronic block diagram on Fig. 4).

The proton solid angle is defined by the S_1 counter and is 0.0021 sr. The Čerenkov counter has a solid angle of 0.021 sr; its geometrical efficiency, averaged over target size, is 84% for Compton events and 7.5% for π^0 events. This geometry has been chosen in order to reduce π^0 background as much as possible and to get a good Compton π^0 background separation. However, as we are measuring a ratio between cross sections, geometrical efficiencies will not affect the final result. Moreover, in the course of the experiment, we have lost a fraction of the more energetic protons (~20% of the total). In fact, the dE/dx values for protons and pions are well separated at counter S_1 (because it is followed by more absorber), while for counter S_2 there is a partial overlap. In order to achieve an efficient pion rejection we have set the S_2 voltage at a relatively low value so that we lose in S_2 a fraction of the protons with lower dE/dx or, equivalently, with higher energy. However, this is of no importance for us, first, because we are primarily interested in the less energetic protons coming from the polarized γ spectrum region, and second, because we are measuring a ratio between the counting rates.

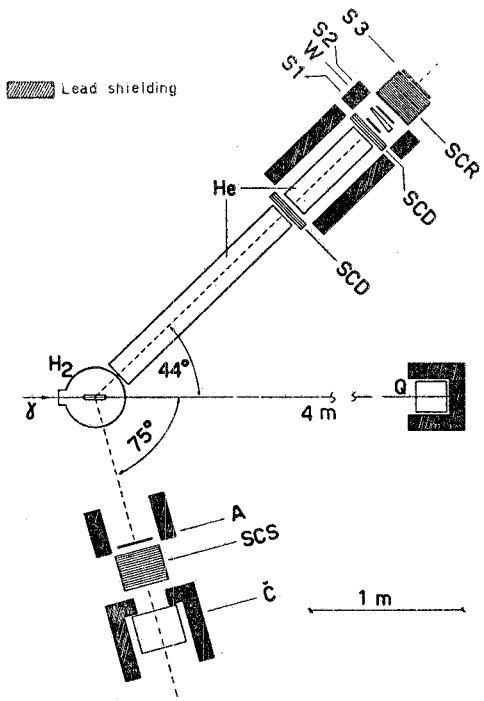

FIG. 3. Experimental apparatus. Symbols are as follows: *SCD*: thin-plate directional spark chamber; *SCR*: range spark chamber; S_1, S_2, S_3: plastic scintillators; W: wedge-shaped aluminum absorber; A: veto plastic scintillator; *SCS*: shower spark chamber; $\check{C}$: integral lead-glass Čerenkov counter; Q: Wilson quantameter.

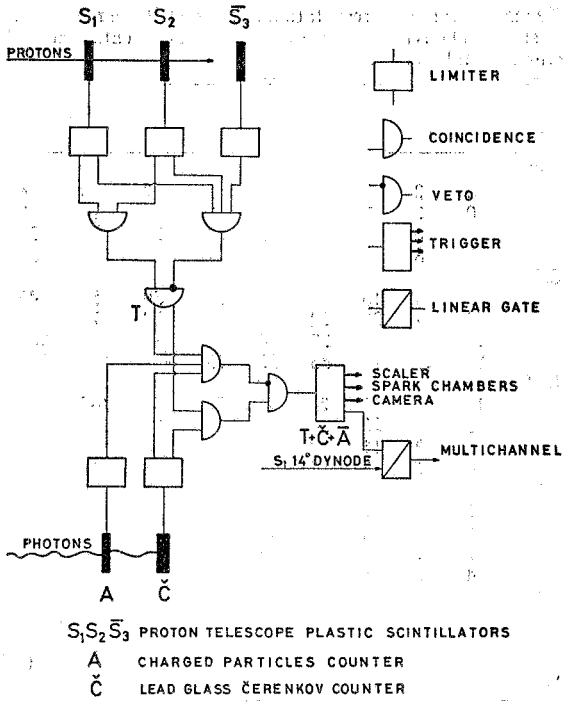

FIG. 4. Electronic block diagram.

The energy intervals for the primary photons which contribute to the two reactions are shown in Fig. 2. The spectrum position has been chosen so that the π^0 zone falls on the low-intensity region and the Compton on the high one. In such a way we may reduce by a factor ~2 the ratio of the π^0 background to the Compton yield, in comparison with the use of a conventional bremsstrahlung spectrum.

IV. DATA REDUCTION

All our events have been divided into two energy intervals:

interval I: $300 \leq K \leq 335$ MeV,

interval II: $335 \leq K \leq 370$ MeV,

where K is the primary photon energy (calculated according to Compton kinematics). It must be emphasized that there is a 50-MeV energy separation between incoming photons that contribute to the Compton effect and those that contribute to π^0 photoproduction (with

TABLE I. Matrix representation of the distribution of events versus $\Delta\theta$, $\Delta\varphi$. $N_{\parallel}$ and $N_{\perp}$ refer to data collected with the two polarization states. The $N_{\parallel}$ matrix shown is the experimental one multiplied by a factor 0.95 in order to normalize at equal (beam dose×good pictures)/total pictures.

$N_{\parallel}$ ($300 \leqslant K \leqslant 335$ MeV)

$\Delta\varphi$																				
−6.9°	5	2	0	5	2	5	2	5	6	5	10	8	5	3	4	5	6	1	3	2
	0	2	8	4	8	8	12	11	8	19	15	18	15	20	12	15	10	8	2	5
	5	6	6	13	13	24	22	26	27	29	24	30	34	30	27	22	18	13	9	3
	5	8	10	19	28	17	29	36	36	60	43	39	48	40	36	21	19	16	10	1
−3.3°	3	9	15	15	27	26	39	55	47	54	53	50	48	27	31	37	39	17	19	9
	9	17	20	22	37	38	52	70	68	60	74	60	65	42	35	42	31	22	13	10
	10	12	18	29	30	63	85	110	109	120	65	79	51	48	32	36	26	32	13	6
	11	15	17	35	32	75	114	142	179	159	113	86	64	66	46	39	25	20	17	11
0.3°	10	16	17	25	41	73	109	143	198	155	100	87	61	49	37	39	36	32	13	7
	9	16	20	34	39	66	91	114	118	91	88	67	60	48	29	37	30	18	19	10
	7	7	11	17	31	43	48	67	71	66	76	49	47	42	50	33	25	23	16	10
	4	5	18	20	22	38	37	45	46	49	40	48	41	32	30	29	28	22	16	9
3.9°	5	5	12	7	24	30	23	34	53	38	41	47	29	37	29	24	28	15	12	4
	5	4	13	14	17	15	16	32	32	25	26	24	25	29	18	16	20	17	10	4
	2	2	4	8	7	9	14	14	10	25	13	10	13	11	11	15	9	3	5	2
	4	2	1	2	1	8	7	8	7	12	10	10	8	7	9	1	5	2	0	3
7.5°																				
	−10°		−8°		−6°		−4°		−2°		0°		2°		4°		6°		8°	10° $\Delta\theta$

$N_{\perp}$ ($300 \leqslant K \leqslant 335$ MeV)

$\Delta\varphi$																				
−6.9°	0	0	1	4	3	3	9	9	10	4	7	5	5	6	4	7	6	3	5	1
	5	0	6	5	10	15	9	14	16	20	16	20	20	19	13	12	6	9	4	2
	4	6	4	6	17	17	16	40	25	35	39	34	30	30	26	24	13	18	4	4
	3	5	8	21	21	18	27	39	40	50	30	42	42	36	38	30	31	16	9	10
−3.3°	5	7	13	25	30	40	43	49	56	68	65	66	50	55	40	35	26	23	10	18
	8	12	15	19	33	47	55	79	71	72	66	68	68	48	43	42	35	27	22	16
	10	8	19	32	42	66	72	98	125	108	80	81	71	61	49	54	31	25	14	10
	11	13	12	35	28	72	94	147	149	128	118	82	62	71	47	48	27	17	16	9
0.3°	9	16	16	27	56	68	104	152	155	146	106	82	74	63	61	41	40	25	25	14
	4	13	19	23	17	73	74	120	134	122	90	93	68	66	50	45	34	25	17	12
	11	12	21	29	31	39	51	62	93	72	63	73	66	70	40	34	19	26	22	3
	8	10	17	24	21	36	39	46	58	71	61	54	48	52	48	34	32	24	16	10
3.9°	7	5	12	17	21	23	29	39	41	40	42	46	46	39	34	33	26	13	14	12
	2	8	11	11	17	22	26	28	27	31	30	31	34	34	26	25	18	16	14	5
	3	3	5	7	6	8	16	18	11	24	13	22	24	14	16	12	13	11	2	2
	2	3	2	3	4	3	5	13	9	11	14	9	6	9	7	6	4	5	3	2
7.5°																				
	−10°		−8°		−6°		−4°		−2°		0°		2°		4°		6°		8°	10° $\Delta\theta$

the same proton kinematics); thus the π^0 events which are classed in these intervals lie, respectively, in the energy intervals $350 \leq K \leq 385$ MeV, $385 \leq K \leq 420$ MeV. In the first interval we have the maximum of polarization and for this we will give the ratio of cross sections. Results from the second one will be used as a check because we expect here almost equal $C_{\parallel}$ and $C_{\perp}$ counting rates owing to the small value of the polarization. We have collected about 33 000 events, of which ~21 000 lie in the first interval and ~12 000 in the second one.

From the scanning of the pictures of the events we derive the following quantities:

θ_p is the proton angle with respect to the beam,
T_p is the proton kinetic energy,
$\theta_{\gamma S}$ is the photon angle with respect to the beam.

With the formulas of Compton kinematics, we calculate, from θ_p and T_p, the expected photon direction $\theta_{\gamma T}$. Then we define two angular deviations:

$$\Delta\theta = \theta_{\gamma T} - \theta_{\gamma S}$$

and $\Delta\varphi$, the angle between planes (**K**,**p**) and (**K**,**K′**); **K** is the beam direction, **p** is the proton direction, and **K′** is the final photon direction.

Notice that if we ignore the scattering of the recoil proton, we have $\Delta\theta = \Delta\varphi = 0$ for Compton events, while for π^0, $\Delta\theta$, and $\Delta\varphi$ we can assume any values compatible with our geometry. Therefore if we plot the events against $\Delta\theta$ and $\Delta\varphi$, the Compton events are contained in a Gaussian-like peak around $\Delta\theta = \Delta\varphi = 0$ whose width is primarily due to the proton scattering. This peak will be superimposed on the distribution of π^0 events,

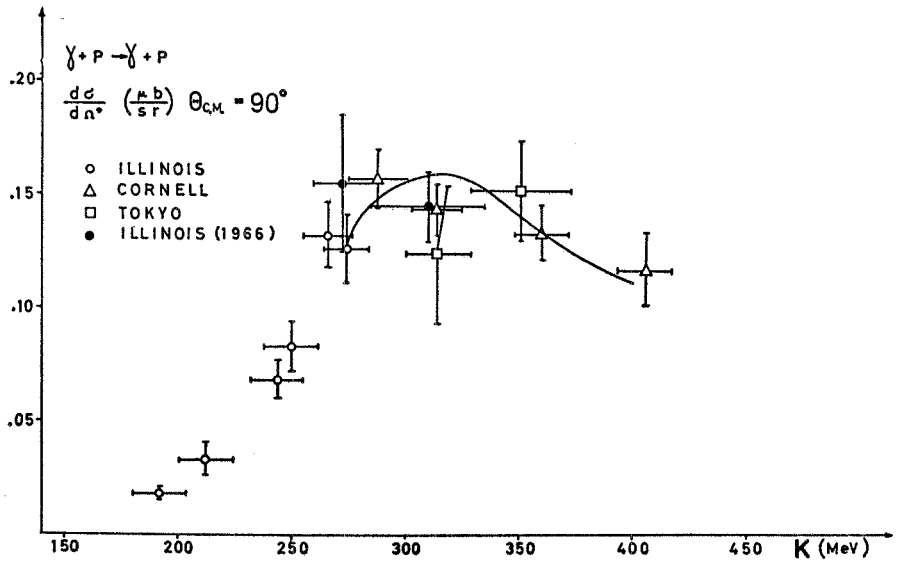

FIG. 5. Experimental values for 90° c.m. Compton cross sections taken from Refs. 4–7. The curve shown has been used for Monte Carlo calculations.

which is flatter and wider. In Table I we present two $\Delta\theta$, $\Delta\varphi$ matrices which show the experimental distribution for the two polarizations. The Compton peak is not centered at 0° because of small errors in the measurement of the spark-chamber position.

As an aid to the analysis of the experimental distributions of $\Delta\theta$ and $\Delta\varphi$, these were also calculated by means of a Monte Carlo method. In this method the experimental conditions are simulated as accurately as possible, using as inputs the experimental spectrum and the known cross sections for Compton effect and π^0 photoproduction; account has been taken of target size, of the proton scattering, and, approximately, of edge effects in shower detection. [The experimental values of interest for Compton[4–7] (π^0 photoproduction[8]) unpolarized cross sections and the interpolating curves used for Monte Carlo calculations are shown in Figs. 5 and 6. Polarized π^0 cross sections were then calculated using the asymmetry measurements reported in Ref. 9.] Because of limited computer time, the Monte Carlo simulated events are slightly less numerous than the experimental ones. Therefore in the following, when necessary, the Monte Carlo predictions are accompanied by their statistical error.

We have used the Monte Carlo results in the data analysis in the following way. We assume that the Monte Carlo method predicts correctly the shape of the $\Delta\theta$-$\Delta\varphi$ distribution, for both π^0 and Compton events. Then the experimental distribution should be obtained by a linear combination of the two predicted ones. Requiring that this combined distribution and the experimental one contain the same number of events, we are left with only one free parameter which may be chosen to be the total number of Compton events. Then we have varied this parameter and we have made a χ^2 test comparing the experimental and Monte Carlo distributions. We find the value of the parameter for which the χ^2 attains the minimum and correspondingly we obtain the separation of the experimental events between π^0 and Compton events. This

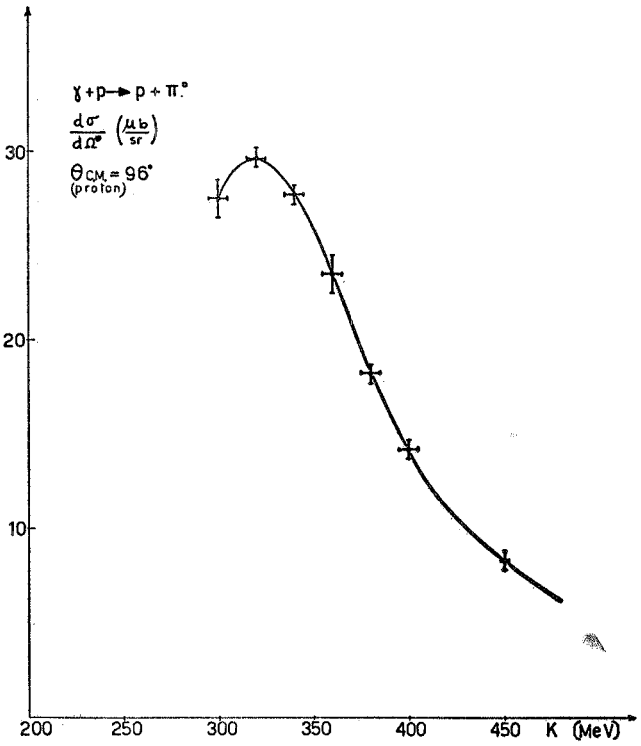

FIG. 6. Experimental values for π^0 photoproduction cross sections at $\theta_p = 96°$ c.m. Data are taken from Ref. 8. The curve shown has been used for Monte Carlo calculations.

[4] G. Bernardini *et al.*, Nuovo Cimento 18, 1203 (1960).
[5] J. W. De Wire *et al.*, Phys. Rev. 124, 909 (1961).
[6] Y. Nagashima, Ph.D. thesis, Tokyo, 1964 (unpublished).
[7] E. R. Gray, Ph.D. thesis, Urbana, Ill., 1966 (unpublished).
[8] J. T. Beale *et al.*, Caltech Report No. CTSL-42, 1966 (unpublished).
[9] A. Donnachie and G. Shaw, Ann. Phys. (N. Y.) 37, 333 (1966)

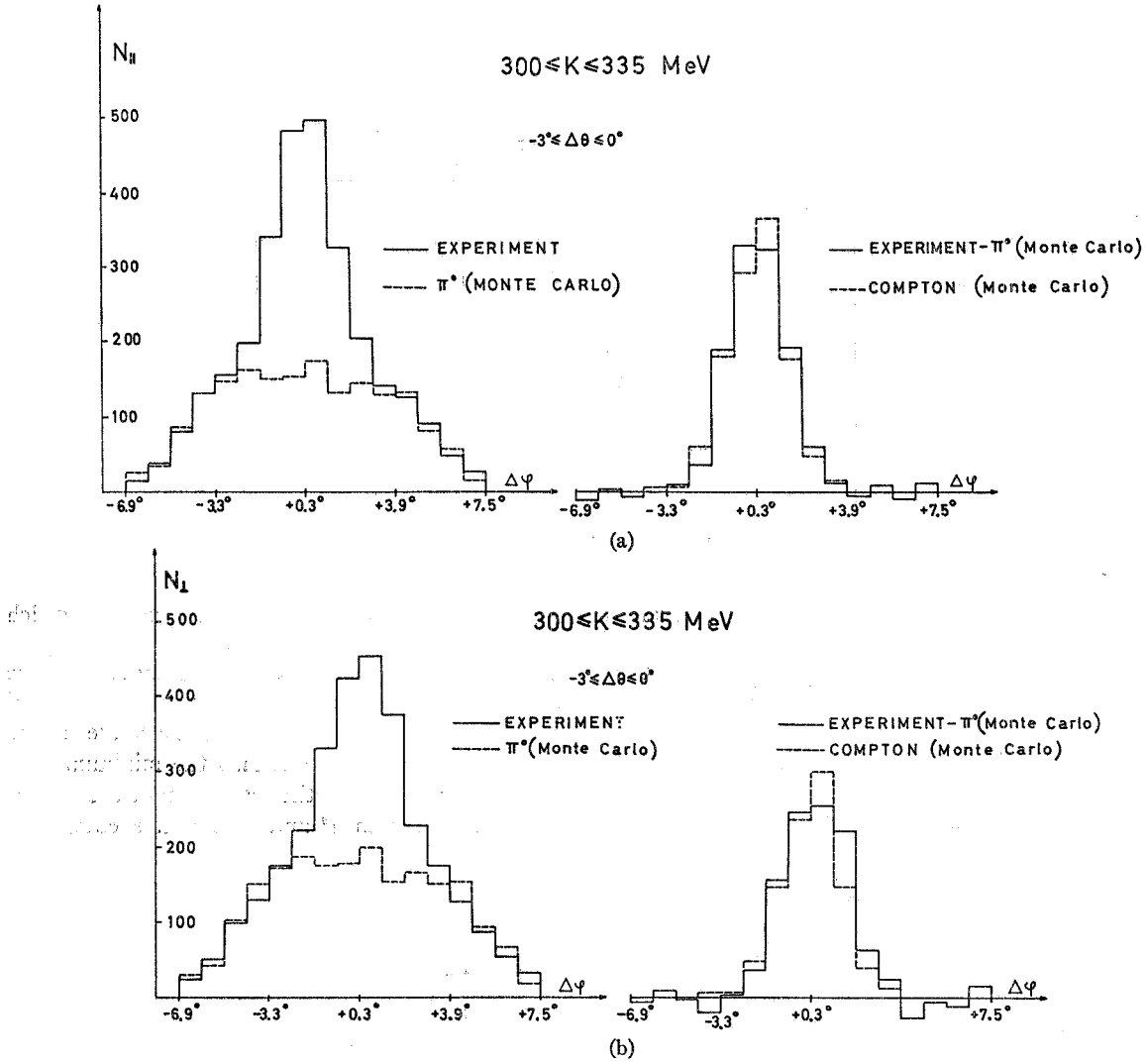

FIG. 7. Distribution versus $\Delta\varphi$ of the events having $-3°\leqslant\theta\leqslant 0°$ (this interval is chosen in order to be centered at the maximum of the Compton peak; it contains about 60% of all Compton events). On the left-hand side the full line represents the experimental data, and the dashed line the π^0 background estimated using the Monte Carlo technique. Subtracting this background one obtains, for the distribution of the Compton events, the full-line histogram shown on the right-hand side. There the dashed line represents the Monte Carlo prediction for Compton events.

comparison has been carried out in the region $-6.9°\leq\Delta\varphi\leq+7.5°$, $-7°\leq\Delta\theta\leq+5°$ of the matrices of Table I for each matrix number (except the cases with less than 20 events which were grouped together). The fit is statistically acceptable because the χ^2 values obtained are the following:

$N_{\parallel}$: $(\chi^2)_{\min}=161$, 157 degrees of freedom;

$N_{\perp}$: $(\chi^2)_{\min}=156$, 159 degrees of freedom.

The remaining events of the matrix have not been considered because of systematic deviations of the Monte Carlo predictions for the tails of the distribution in $\Delta\theta$. In any case the number of Compton events in this region is surely negligible. The results of such a procedure are shown in Figs. 7(a) and 7(b) for a central section of the distribution made along the $\Delta\varphi$ axis.

The separation between Compton and π^0 events has also been carried out independently of the Monte Carlo calculation by graphically extrapolating the background shape from the region external to the peak to the region under the peak. This has been done in several ways, analyzing various sections of the distribution both in $\Delta\theta$ and $\Delta\varphi$. This is shown in Figs. 8(a) and 8(b), in which are presented the central sections of the distributions made along $\Delta\theta$. In Figs. 8(c) and 8(d) we report, for purposes of comparison, the sum of the two diamond distributions: the experimental one and the prediction of the Monte Carlo calculation.

The separation of the Compton events from the π^0 events is not free of uncertainties, owing to the peculiar shape of the $\Delta\theta$-$\Delta\varphi$ distribution, which is the sum of the bell-shaped curves of different width. In effect the use

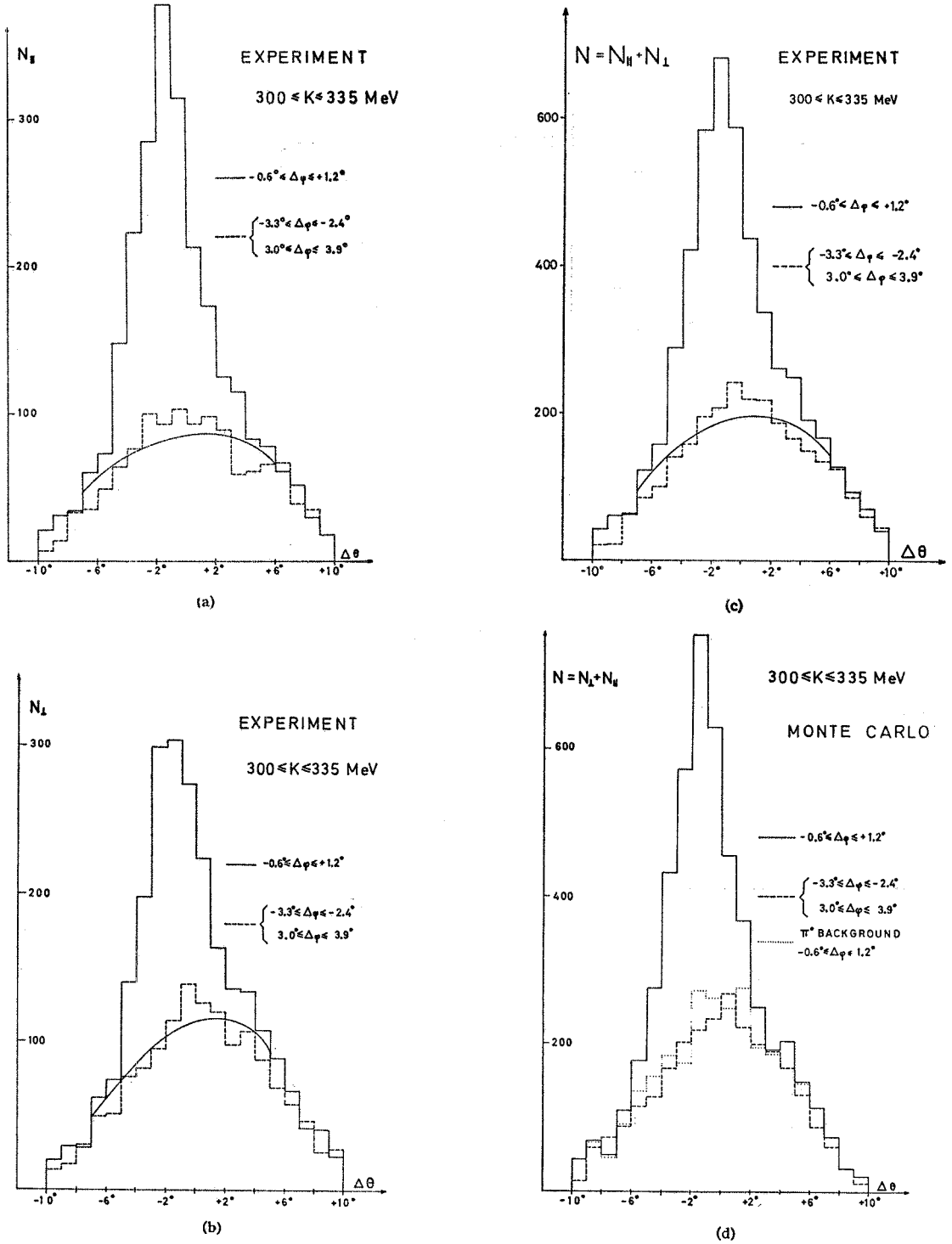

FIG. 8. (a)–(c): Distribution versus $\Delta\theta$ of the events having $-0.6° \leqslant \Delta\varphi \leqslant +1.2°$ (full-line histogram) and of the events having $-3.3° \leqslant \Delta\varphi \leqslant -2.4°$ and $3.0° \leqslant \Delta\varphi \leqslant 3.9°$ (dashed-line histogram). The full-line histogram passes through the Compton peak, while the dashed one contains almost only background. We report it to give an idea of the background behavior. The smooth curve represents the assumed background behavior. In (d) are presented the corresponding histograms predicted by the Monte Carlo calculation together with the predicted π° background under the peak.

of the Monte Carlo calculation leads to a smaller number of Compton events than the direct background extrapolation. The ambiguity is essentially due to the background level under the Compton peak. However, neither varying the criteria of comparison of the data with the Monte Carlo calculation, nor following differ-

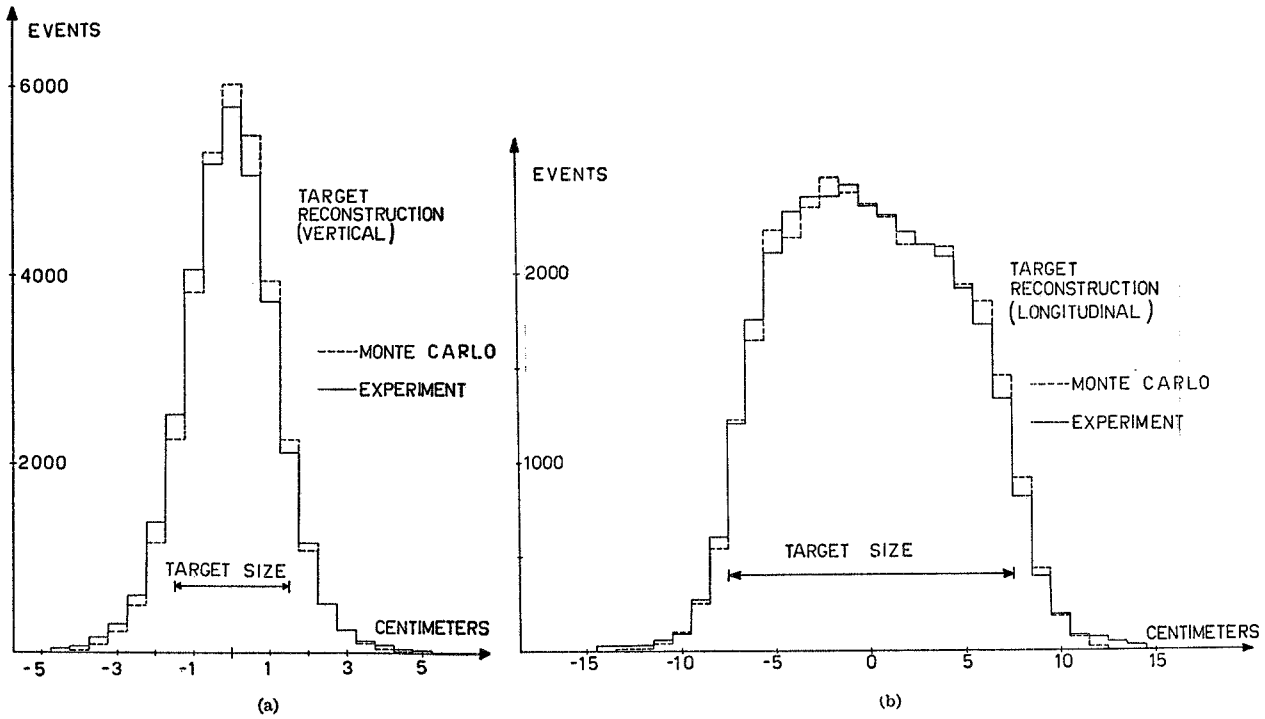

FIG. 9. Distribution in the median vertical plane of the target of the interaction points, as reconstructed from the scanning of the photographs. Figure 9(a) refers to the vertical distribution and Fig. 9(b) to the one along the beam axis. Dashed lines represent the Monte Carlo predictions.

ent suggestions for the background extrapolation, makes much difference in the final result ($C_{\parallel}/C_{\perp}$ ratio) if one takes care to follow the same criteria in making the separation of the data relative to the two diamonds. A greater $\Delta\theta$-$\Delta\varphi$ acceptance of our apparatus would probably have made slightly easier the π^0-Compton separation but would have also required a larger scanning time because of the increased yield of π^0 events.

From the scanning we get also the coordinates of the interaction point in the target. In Figs. 9(a) and 9(b) we show their distribution along the vertical and the longitudinal (parallel to beam) direction together with the curves predicted by the Monte Carlo calculation.

V. RESULTS

We first discuss the results obtained for the polarized region, i.e., $300 \leq K \leq 335$ MeV for Compton events, to which corresponds the interval $350 \leq K \leq 385$ MeV for π^0 events. For Compton events the value of the polarization averaged over this interval is $P=0.276$. As said before, we assume that the error on the polarization is $\Delta P=0.01$; however, taking into account the fact that possible errors in the position of the interval of the accepted energies may lead to errors in the calculation of the average polarization, we take a slightly larger error on P and write

$$P=0.276\pm0.014.$$

Using the Monte Carlo results as described before, we find

$$C_{\parallel}=1975\pm70, \quad \pi_{\parallel}{}^0=8170\pm100,$$
$$C_{\perp}=1620\pm60, \quad \pi_{\perp}{}^0=9255\pm 95.$$

The errors are statistical in nature and include both the counting statistical error and the statistical uncertainty in setting the level of the π^0 background. They are computed following the formulas given by Moravcsik and Cziffra[10] for the errors on the coefficients when using the least-squares method. All these numbers refer to the same dose. For the ratio we then obtain

$$R_c=C_{\parallel}/C_{\perp}=1.22\pm0.06.$$

Using the direct extrapolation of the background, we get for $C_{\parallel}$ and $C_{\perp}$ higher numbers:

$$C_{\parallel}\cong2450, \quad C_{\perp}\cong2030,$$

and a ratio $C_{\parallel}/C_{\perp}=1.21$ which is in agreement with the previous one. We stress here again the fact that the uncertainty on the exact background shape may lead to rather large errors on the absolute yields of $C_{\parallel}$ and $C_{\perp}$; however, if one takes care to use the same criteria for both the $\parallel$ and $\perp$ distributions, the influence of the systematic error due to background overestimation or underestimation is small on the ratio R_c. Inserting the value of R_c in formula (1) together with the value of the

[10] P. Cziffra and M. J. Moravcsik, University of California Radiation Laboratory Report No. UCRL 8523 (unpublished).

averaged polarization, we get

$$R_\sigma = 2.1_{-0.4}^{+0.5},$$

where the errors are computed quadratically combining the errors due to R_c and P (this last one is, however, less important).

A. Consistency Checks

Summing the results of both diamonds, we get the over-all background-to-Compton ratio

$$\frac{\pi^0}{C} = \frac{\pi_{11}^0 + \pi_\perp^0}{C_{11} + C_\perp} = 4.85 \pm 0.15.$$

The quoted error is only the statistical one. Here systematic errors in background separation are very important. The Monte Carlo prediction for it is 5.2 ± 0.15 and has been calculated using the value for the cross sections shown in Figs. 5 and 6. The partial disagreement could also be due to an inappropriate choice of the curve fitting the measured Compton cross sections whose behavior at the resonance is not well known since the experimental data have large errors. Also, the π_{11}^0 and $\pi_\perp^0$ counts show an asymmetry due to the presence of a slight polarization in the region $350 \leq E_\gamma \leq 385$ MeV. We recall that for π^0 photoproduction the asymmetry is in the opposite direction with respect to the Compton effect and its value is $d\sigma_\perp/d\sigma_{11} \cong 4$ at the resonance. Inserting in the Monte Carlo calculation the known π^0 asymmetry,[9] we obtain $\pi_\perp^0/\pi_{11}^0 = 1.12 \pm 0.05$, which is in excellent agreement with the experimental result

$$\pi_\perp^0/\pi_{11}^0 = 1.13 \pm 0.02.$$

For the low-polarization region ($335 \leq K \leq 370$ MeV for Compton, $385 \leq K \leq 420$ MeV for π^0 events) the data analysis was carried on in the same way and here we quote the results obtained using the Monte Carlo method:

$$C_{11} = 800 \pm 50, \quad \pi_{11}^0 = 5160 \pm 75,$$
$$C_\perp = 750 \pm 45, \quad \pi_\perp^0 = 5390 \pm 70.$$

The experimental ratios are therefore the following:

$$C_{11}/C_\perp = 1.07 \pm 0.09, \quad \pi_\perp^0/\pi_{11}^0 = 1.045 \pm 0.020,$$

while the Monte Carlo predictions are

$$\pi_\perp^0/\pi_{11}^0 = 1.05 \pm 0.05.$$

The ratio $C_{11}/C_\perp$ is near to 1, as expected from the low value of the polarization.

B. Comparison with Theory

We show in Fig. 10 our experimental value of $d\sigma_{11}/d\sigma_\perp$ together with some theoretical curves. Curves

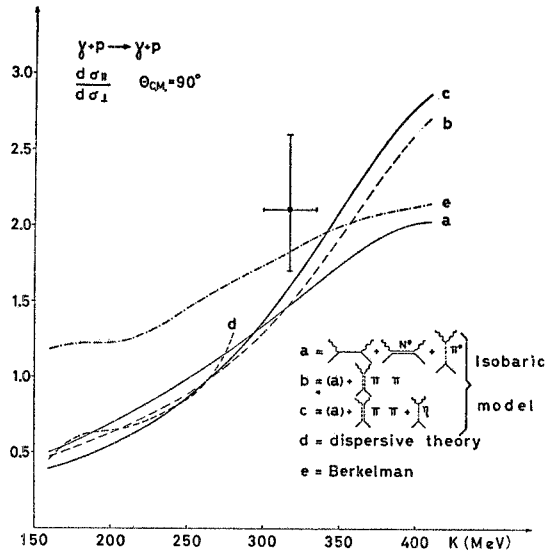

FIG. 10. Our experimental result is compared to various theoretical curves. Curves (a)–(c) have been calculated by us with the isobaric model following Ref. 9. Curve (d) is taken from Ref. 11 and curve (e) from the Berkelman work (Ref. 14).

(a), (b), and (c) refer to calculations based on an isobaric model used by Nagashima,[11] considering contributions from various intermediate states. Curve (d) is the prediction of dispersion theory,[12,13] whose range of validity, however, ends near 270 MeV. We reproduce it to show that the more refined calculations based on dispersion theory give results not in disagreement with the simple isobaric model. Curve (e) is derived from the Berkelman phenomenological model.[14] Assuming[15] that the only multipole contributing to the transition is the magnetic dipole M_{1+}, one gets $d\sigma_{11}/d\sigma_\perp = 2.5$.

ACKNOWLEDGMENTS

We would like to mention here that in the preliminary part of the work Professor G. Diambrini and Professor G. Bologna kindly collaborated with us. We thank Professor G. Bologna also for giving us the program for the spectrum calculation, and Dr. F. Fabbri for help in the calculations. Thanks are due to the Synchrotron staff for assistance during the machine runs and to the Istituto Superiore di Sanità for computer time. Finally, we are indebted to G. Di Stefano and co-workers for their excellent technical work.

---

[11] Y. Nagashima, Progr. Theoret. Phys. (Kyoto) 33, 828 (1965).
[12] M. Jacob and J. Mathews, Phys. Rev. 117, 854 (1960).
[13] A. Santroni, Genova University, Report No. 66/2 A. E. B.-11, 1966 (unpublished).
[14] K. Berkelman, Nuovo Cimento 21, 633 (1961).
[15] A. Verganelakis, Nuovo Cimento 31, 1121 (1964).